Switch in FGFR3 and -4 Expression Profile During Human Renal Development May Account for Transient Hypercalcemia in Patients With Sotos Syndrome due to 5q35 Microdeletions

Henricus A. M. Mutsaers, Elena N. Levtchenko, Laetitia Martinerie, Jeanne C. L. M. Pertijs, Karel Allegaert, Koenraad Devriendt, Rosalinde Masereeuw, Leo A. H. Monnens, and Marc Lombès

Institut National de la Santé et de la Recherche Médicale (H.A.M.M., L.M., M.L.), Unité 693, Faculté de Médecine Paris-Sud, 94276 Le Kremlin-Bicêtre, France; PremUP Foundation (L.M., M.L.), 75014 Paris, France; Departments of Pharmacology and Toxicology (H.A.M.M., J.C.L.M.P., R.M.), Physiology (L.A.H.M.), Radboud University Medical Center, 6525 GA Nijmegen, The Netherlands; and Departments of Pediatrics and Growth and Regeneration (E.N.L., K.A.) and Center for Human Genetics (K.D.), University Hospitals Leuven and Katholieke Universiteit Leuven, 3000 Leuven, Belgium

Context: Sotos syndrome is a rare genetic disorder with a distinct phenotypic spectrum including overgrowth and learning difficulties. Here we describe a new case of Sotos syndrome with a 5q35 microdeletion, affecting the fibroblast growth factor receptor 4 (*FGFR4*) gene, presenting with infantile hypercalcemia.

Objective: We strove to elucidate the evanescent nature of the observed hypercalcemia by studying the ontogenesis of FGFR3 and FGFR4, which are both associated with fibroblast growth factor (FGF) 23-mediated mineral homeostasis, in the developing human kidney.

Design: Quantitative RT-PCR and immunohistochemical analyses were used on archival human kidney samples to investigate the expression of the FGFR signaling pathway during renal development.

Results: We demonstrated that renal gene and protein expression of both FGFRs increased during fetal development between the gestational ages (GAs) of 14–40 weeks. Yet *FGFR4* expression increased more rapidly as compared with *FGFR3* (slope 0.047 vs 0.0075, $P = .0018$). Moreover, gene and protein expression of the essential FGFR coreceptor, Klotho, also increased with a significant positive correlation between *FGFR* and *Klotho* mRNA expression during renal development. Interestingly, we found that perinatal *FGFR4* expression (GA 38–40 wk) was 7-fold higher as compared with *FGFR3* ($P = .0035$), whereas in adult kidney tissues, *FGFR4* gene expression level was more than 2-fold lower compared with *FGFR3* ($P = .0029$), thus identifying a molecular developmental switch of FGFR isoforms.

Conclusion: We propose that the heterozygous *FGFR4* deletion, as observed in the Sotos syndrome patient, leads to a compromised FGF23 signaling during infancy accounting for transient hypercalcemia. These findings represent a novel and intriguing view on FGF23 mediated calcium homeostasis. **(*J Clin Endocrinol Metab* 99: E1361–E1367, 2014)**

Sotos syndrome is an autosomal dominant disorder characterized by overgrowth, learning disability, and distinctive facial features such as macrocephaly (1, 2). The syndrome results from mutations and deletions, mostly de novo, of the *NSD1* gene located at chromosome 5, which encodes for the nuclear receptor-binding SET (Su(var)3-9,

ISSN Print 0021-972X ISSN Online 1945-7197
Printed in U.S.A.

Received January 15, 2014. Accepted March 14, 2014.
First Published Online March 26, 2014

Abbreviations: FGF, fibroblast growth factor; FGFR, FGF receptor; GA, gestational age; NSD1, nuclear receptor-binding SET (Su(var)3,9, Enhancer-of-zeste, Trithorax)-domain containing protein 1; qPCR, quantitative PCR.

Enhancer-of-zeste, Trithorax) domain containing protein 1 (NSD1). Little is known regarding the function of NSD1, and it remains unclear how the *NSD1* gene inactivation or NSD1 dysfunction may cause the Sotos phenotype (3). Intragenic mutations are responsible for 80%–85% of Sotos syndrome cases, whereas 5q35 microdeletions encompassing *NSD1* cause 10%–15% of the cases in Europe and the United States (4). Of note, 5q35 microdeletions vary in size, from 0.4 to 5 Mb and may affect genes flanking *NSD1* (5). Saugier-Veber et al (6) mentioned the occurrence of nephrocalcinosis in three patients with large deletions and suggested the presence of a predisposing gene in the deleted area. This phenotype spectrum was confirmed by Kenny et al (7), who reported two unrelated cases of Sotos syndrome associated with nephrocalcinosis, one of whom had proven infantile hypercalcemia. The authors suggested that the heterozygous deletion of *SLC34A1*, encoding the main sodium phosphate cotransporter NPT2a, could explain the temporary hypercalcemia in these patients. However, hypercalcemia was absent in patients with a loss of function of sodium-phosphate transport protein 2a, as described by Magen et al (8), in contrast to $Npt2^{-/-}$ mice that exhibited a slight but significant increase in serum calcium concentration compared with wild-type mice (9). Thus, the transient nature of the hypercalcemia remains unexplained in Sotos syndrome patients.

Another gene mapped to the deletion interval is *FGFR4*, encoding for the fibroblast growth factor receptor (FGFR) 4. The fibroblast growth factors (FGFs) are a large family of peptides that are involved in a myriad of biological processes, including development and mineral homeostasis (10). Currently seven FGF subfamilies have been identified encompassing 22 different FGFs. The FGF19 subfamily, containing FGF19, FGF21, and FGF23, plays a key role in regulating energy and mineral metabolism (10). Of interest, FGF23 is of the utmost importance in maintaining vitamin D, phosphate, and calcium levels (11). FGF23 is a ligand for several FGFRs (eg, FGFR1, FGFR3, and FGFR4), and it has been demonstrated that Klotho forms a complex with these receptors, resulting in an increased affinity selectively to FGF23 (10, 12). FGFR1 is implicated in the FGF23 effects on NPT2a and NPT2c cotransporters (13), whereas FGFR3 and FGFR4 are linked to FGF23 effects on vitamin D and calcium levels (14). Thus, there is a clear link between FGFR4-mediated FGF23 signaling and calcium homeostasis. Here we describe a new Sotos syndrome case, due to a 5q35 microdeletion, with infantile hypercalcemia, and we hypothesized that a heterozygous mutation in *FGFR4* might be a possible explanation for the observed elevated calcium levels. To unravel the temporary characteristics of the perceived hypercalcemia, we studied FGFR3 and FGFR4 ontogenesis in the human developing kidney that has never been reported to date.

Materials and Methods

Ethics statement

Fetal samples were collected after parental informed and written consent and after declaration to the French Biomedical Agency (Decree 003812, September 22, 2006). Archival formol-fixed, paraffin-embedded fetal and neonatal kidneys were selected from the collections of several departments of pathology according to the French legislation. Parental informed and written consents had been obtained at the time of tissue collection and were conserved in each department. Experimental use of these samples has been declared to the French Biomedical Agency (Decree 003812, September 22, 2006).

Human renal samples

Snap-frozen kidney samples from 18 fetuses, with a gestational age of 14–40 weeks, obtained from the Department of Fetopathology of Robert-Debré University Hospital (Paris, France) were used for quantitative PCR (qPCR). For histology, a selection was made from 37 archival tissue sections previously checked for quality and integrity by immunostaining with vimentin and low-molecular-weight cytokeratin (15).

Quantitative PCR

To study gene expression, total RNA (1 μg) was reverse transcribed using 50 U MultiScribe reverse transcriptase (Life Technologies). Subsequently, cDNA was used for qPCR performed with a StepOnePlus real-time PCR system using the TaqMan universal PCR master mix (Life Technologies). *GAPDH* was used as housekeeping gene, and relative mRNA expression levels were calculated using the equation, $(2^{-\Delta CT})100$, or as fold change using the $2^{-\Delta\Delta CT}$ method. The following primer-probe sets were used: *FGFR3*, Hs00179829_m1; *FGFR4*, Hs01106908_m1; *GAPDH*, Hs99999905_m1; and *Klotho*, Hs00183100_m1 (all obtained from Life Technologies).

Immunohistochemistry

Five-micrometer-thick tissue sections were deparaffinized and rehydrated in successive baths of xylene and graded alcohols. Afterward, the slides were heated in sodium citrate buffer (pH 6) at 100°C for 15 minutes. Endogenous peroxidase was blocked with 3% (vol/vol) H_2O_2 for 30 minutes. Next, nonspecific epitopes were blocked for 30 minutes at room temperature with 1% (w/vol) BSA in PBS containing 0.1% (vol/vol) Tween-20. Subsequently, the slides were incubated overnight at 4°C with rabbit-α-FGFR3 (1:1000; ab137084; Abcam), rabbit-α-FGFR4 (1:500; ab41948; Abcam), or rabbit-α-Klotho (1:100; ab181373; Abcam) in a blocking buffer. To reveal bound Ig, slides were incubated for 30 minutes at room temperature with the ImmPRESS antirabbit Ig kit (Vector), and liquid diaminobenzidine plus chromogene (Dako) was used for visualization. Slides were counterstained with Mayer's hematoxylin and mounted using Glycergel (Dako). Sections were studied via bright-field microscopy (Olympus BX61), and images were taken by means of a Retiga-2000R Fast 1394 digital camera (QImaging).

Statistics

Statistics were performed using GraphPad Prism version 6.03 via a one-way ANOVA followed by Bonferroni's multiple comparison test or an unpaired Student's *t* test. Differences between groups were considered to be statistically significant when $P < .05$. The software was also used to perform linear regression analyses and correlation analyses (Pearson and Spearman).

Results

Case report of a new Sotos syndrome patient with 5q35 microdeletion and infantile hypercalcemia

Subject G was the fourth child of nonconsanguineous parents. His birth weight was 3580 g after 39 weeks of an uncomplicated pregnancy. A short period of artificial ventilation was required after birth due to respiratory distress. Because of dysmorphic features, an array comparative genomic hybridization was performed, which revealed a microdeletion at 5q35, including both *NSD1* and *FGFR4*, as shown in Figure 1A. The deletion was absent in both parents, suggesting that it occurred de novo. In addition, hypercalcemia was observed during the first 2 weeks of life, as presented in Figure 1B, and normalized afterward.

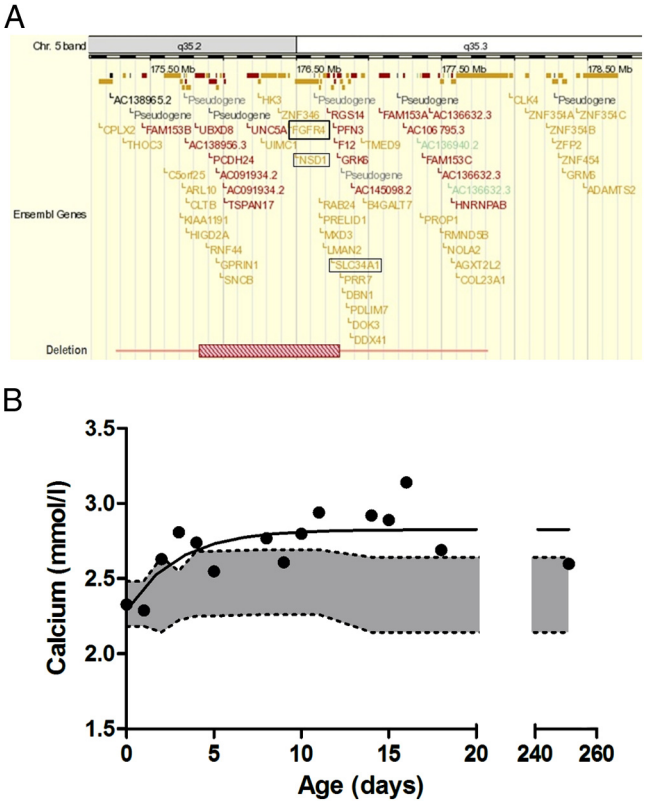

Figure 1. New Sotos syndrome case with infantile hypercalcemia. A, Extent of 5q35 microdeletion including both *NSD1* and *FGFR4*. B, Dots represent the calcium level per day during the first weeks of life. Gray area depicts the normal range of total serum calcium in healthy neonates, adapted from *Roberton's Textbook of Neonatology* (4th ed, 2005, Elsevier Churchill Livingstone).

In the first weeks after birth from day 8 to day 18, serum phosphate levels were slightly reduced ranging from 1.22 to 2.54 mmol/L, with a median value of 1.90 (n = 8) (reference range 1.74–2.66 mmol/L) and returned to normal concentrations afterward. The maximum phosphate reabsorption rate was decreased, possibly due to the heterozygous deletion of solute carrier family 34 (type II sodium/phosphate contransporter), member 1 gene (*SLC34A1*) also lost with the deletion (Figure 1A) (16). During the first 4 days, the child received iv nutrition and was then switched to breast-feeding. At 4 years of age, he was more extensively investigated, and it was demonstrated that serum calcium and PTH levels were normal, whereas 1,25-dihydroxycholecalciferol (ie, active vitamin D) was slightly elevated (86 ng/L, normal range 20–80 ng/L). Nephrocalcinosis was absent on ultrasound scanning. We hypothesized that the heterozygous deletion in *FGFR4* might be the possible explanation for the observed transient elevated calcium levels.

Expression profile of FGFRs during fetal renal development

To elucidate the impact of the observed *FGFR4* deletion as well as the transient infantile hypercalcemia, we studied the renal ontogenesis of FGFRs involved in calcium homeostasis. Figure 2A demonstrates that the gene expression levels of both *FGFR3* and *FGFR4* in kidney samples significantly and positively correlate with gestational age (GA) with a calculated Pearson r of 0.63 ($P = .0054$) and 0.72 ($P = .0008$), respectively. Moreover, the expression level of both receptors steadily increases during renal development from 14 to 40 gestational weeks; yet there is a strikingly greater increase in *FGFR4* gene expression as compared with *FGFR3* (slope 0.047 vs 0.0075, $P = .0018$). An analogous immunochemical pattern was observed with light microscopy, revealing a similar amount of positively stained tubules at 21 weeks of gestation, whereas at a GA of 40 weeks, FGFR4 protein seems to be more abundantly present as compared with FGFR3 (Figure 2B). Furthermore, in the fetal kidney, FGFR3 protein expression appears to be limited to the distal tubules, with some stainings in the glomeruli as well as the medulla (Figure 2B). In contrast, FGFR4 was detected in both the proximal and distal tubules (especially at 40 gestational wk; Figure 2B) as well as the medulla (Figure 2B), whereas the receptor was absent in the glomeruli.

Correlation between FGFR and Klotho expression

It has been previously reported that Klotho is an essential cofactor for FGF23 signaling (10, 17). As shown in Figure 3, A and B, Klotho mRNA and protein expression increases throughout renal development, with low mRNA

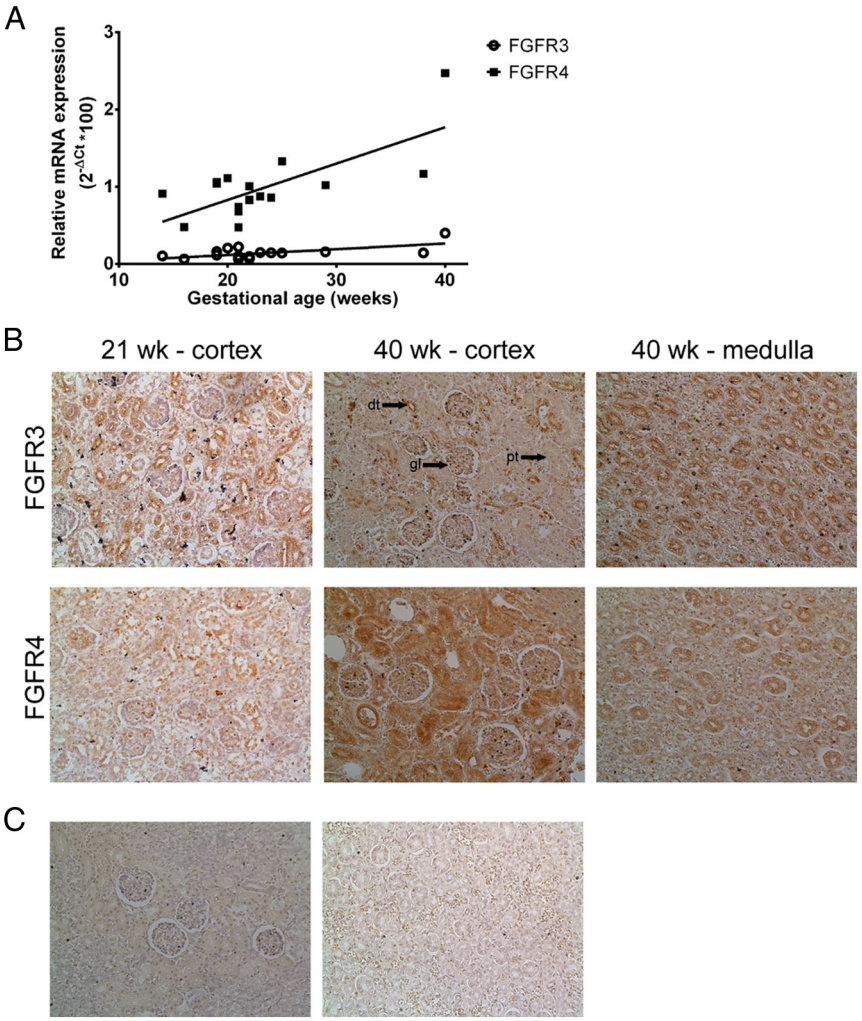

Figure 2. Expression of FGFRs in the human fetal kidney. A, *FGFR* gene expression was studied using RT-qPCR. Relative expression was calculated as $(2^{-\Delta CT})100$. Pearson correlation analysis revealed a significant association between GA and *FGFR3* (○; r = 0.63, $P = .0054$) and *FGFR4* (■; r = 0.72, $P = .0008$) gene expression. B, Immunostaining of FGFRs in the developing kidney. C, Secondary antibody control for FGFR staining. Magnification, ×20. Arrows indicate a typical example of a glomerulus (gl), proximal tubule (pt), and distal tubule (dt).

levels in the fetal kidneys, consistent with the lack of detectable Klotho protein in fetal and neonatal kidney samples, at variance with the adult kidneys, in which Klotho protein is readily detected in renal distal tubules. A significant positive correlation was observed between *Klotho* mRNA and GA (calculated Pearson r = 0.80, $P < .0001$). Moreover, the expression profile of *Klotho* mRNA significantly correlates with both *FGFR3* (r = 0.6, $P = .008$, Figure 3C) and *FGFR4* (r = 0.77, $P = .0002$, Figure 3D) as demonstrated with Spearman correlation analyses, consistent with the key role of Klotho acting as a renal coreceptor for FGF23.

Switch in FGFR expression profile during postnatal development

Next, we compared the FGFR expression profile in fetal, neonatal, and adult kidney samples. As illustrated in Figure 4A, renal *FGFR3* gene expression was extremely low in both the early and late stages of gestation, with a significant 67-fold and 23-fold lower expression of the receptor as compared with the adult level ($P < .0001$). In contrast, renal *FGFR4* mRNA levels were only 5 times lower during early gestation as compared with the adult situation ($P = .004$), whereas there was no significant difference in renal *FGFR4* expression in the late stage of development as compared with adult tissue. Interestingly, during late gestation, relative *FGFR4* expression is 7-fold higher than that of *FGFR3* ($P = .0035$, Figure 4B), whereas in adults, renal *FGFR3* expression level was significantly higher than that of *FGFR4* ($P = .0029$, Figure 4B). At the protein level, immunohistochemical studies revealed a similar trend with more tubules positively stained for FGFR4 than for FGFR3 at 2 and 9 months of age. Moreover, FGFR3 and FGFR4 protein localization was similar in the neonatal kidney as compared with the fetal kidney. Conversely, FGFR3 protein expression was markedly increased in the adult kidney (60 y old) and was detected in proximal and distal tubules as well as glomeruli, whereas there was a strong decline in the number of FGFR4-positive tubules (Figure 4C). These findings indicate a major molecular switch in the respective contribution of both FGFRs in FGF23 signaling during human renal development.

Discussion

Sotos syndrome is a rare genetic disorder characterized by overgrowth, distinct facial features, and learning disabilities. The clinical features of Sotos syndrome vary between cases and seem to be independent of genotype (3). In addition, all features observed in microdeletion cases have also been reported in individuals with intragenic mutations (3). Still, the individuals with 5q35 microdeletions are generally more likely to present with severe learning disabilities and less pronounced overgrowth as compared

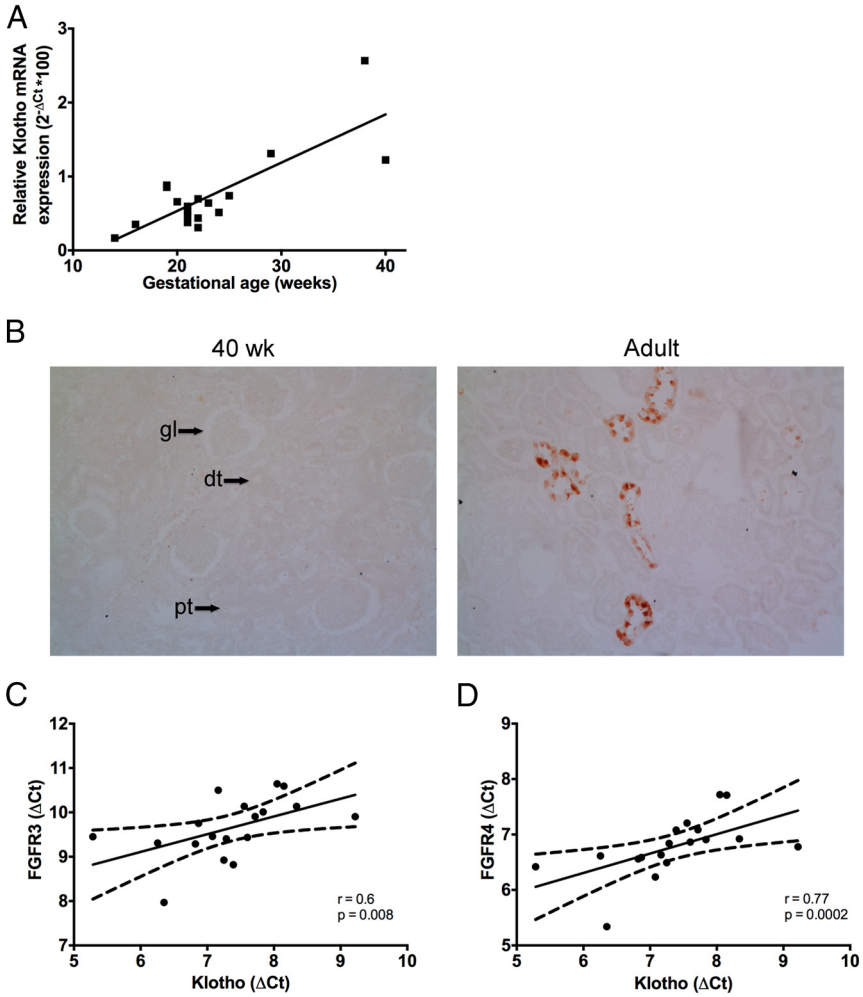

Figure 3. Klotho expression in the developing kidney. *Klotho* and *FGFR* gene expressions were studied using RT-qPCR. A, Relative *Klotho* expression was calculated as $(2^{-\Delta CT})100$. Pearson correlation analysis revealed a significant association between GA and *Klotho* ($r = 0.80$, $P < .0001$). B, Immunostaining of Klotho in fetal (GA of 40 wk) and adult kidney tissue (60 y of age). Magnification, ×20. Arrows indicate a typical example of a glomerulus (gl), proximal tubule (pt), and distal tubule (dt). C, Positive correlation between *Klotho* and *FGFR3* (Spearman $r = 0.6$, $P = .008$). D, Positive correlation between *Klotho* and *FGFR4* (Spearman = 0.77, $P = .0002$).

with patients with intragenic mutations (18). Furthermore, there is a nascent amount of evidence that the phenotypic spectrum also encompasses impaired calcium homeostasis during infancy.

Here we report a new Sotos syndrome case, due to a 5q35 microdeletion, with evanescent hypercalcemia. Because the deletion area included *FGFR4*, we hypothesized that dysfunction of this FGF23 receptor might account for the altered calcium levels. Endocrine calcium homeostasis is an intricate system involving several regulators and feedback loops. During hypocalcemia, PTH is stimulated causing active vitamin D levels to rise, which in turn augments intestinal calcium absorption as well as renal calcium retention (10). In response to elevated serum calcium, osteocyte-produced FGF23 is released. Binding of FGF23 to the FGFR-Klotho complex, including either FGFR3 or FGFR4, inhibits the synthesis of active 1,25 dihydroxyvitamin D3, both directly by reducing 1α-hydroxylase (CYP27B1) expression and increasing expression of the vitamin D degrading enzyme, 24–25 hydroxylase (CYP24) but also indirectly by decreasing PTH levels, resulting in a negative calcium balance (10, 17). Thus, changes in FGF23 signaling will directly impact calcium homeostasis. At present, both FGF23 pathway deficiency and renal FGFR ontogenesis have solely been studied in animal models, and human data are lacking. Therefore, we studied the FGFR3 and FGFR4 expression profile in the developing human kidney.

Our results revealed a molecular switch in the FGFR expression profile during human renal development. These findings provide compelling evidence that heterozygous *FGFR4* inactivation in humans, as observed in a 5q35 microdeletion Sotos syndrome case, might account for an impaired FGF23 signaling pathway during early life, causing transient infantile hypercalcemia. This notion is corroborated by previous animal studies. For instance, Shimada et al (19) reported that calcium levels were elevated in *Fgf23*$^{-/-}$ mice, which is in accordance with the study by Yuan et al (20), and an analogous discovery was made in *Klotho*-deficient mice (21). Hypercalcemia was also observed in *Ffg23* and *Klotho* double-knockout mice (22). Moreover, Haenzi et al (23) described that the loss of Memo, a recently identified FGFR regulator, was associated with increased serum calcium. Of interest, the only phenotypic feature that has been reported in Sotos syndrome cases with microdeletions is nephrocalcinosis (18). Consistent with the transient hypercalcemia observed in the described case, as well as those previously reported (7, 18), it is likely that alterations of calcium homeostasis might be a distinctive feature in Sotos syndrome associated with microdeletions. Moreover, Tatton-Brown et al (5) performed a microsatellite analysis in 33 microdeletion cases and detected a deletion of *FGFR4* in 32 individuals, strengthening the hypothesis that a mutation in *FGFR4*, and subsequent impaired FGF23 signaling, is the culprit in infantile calcium imbalance.

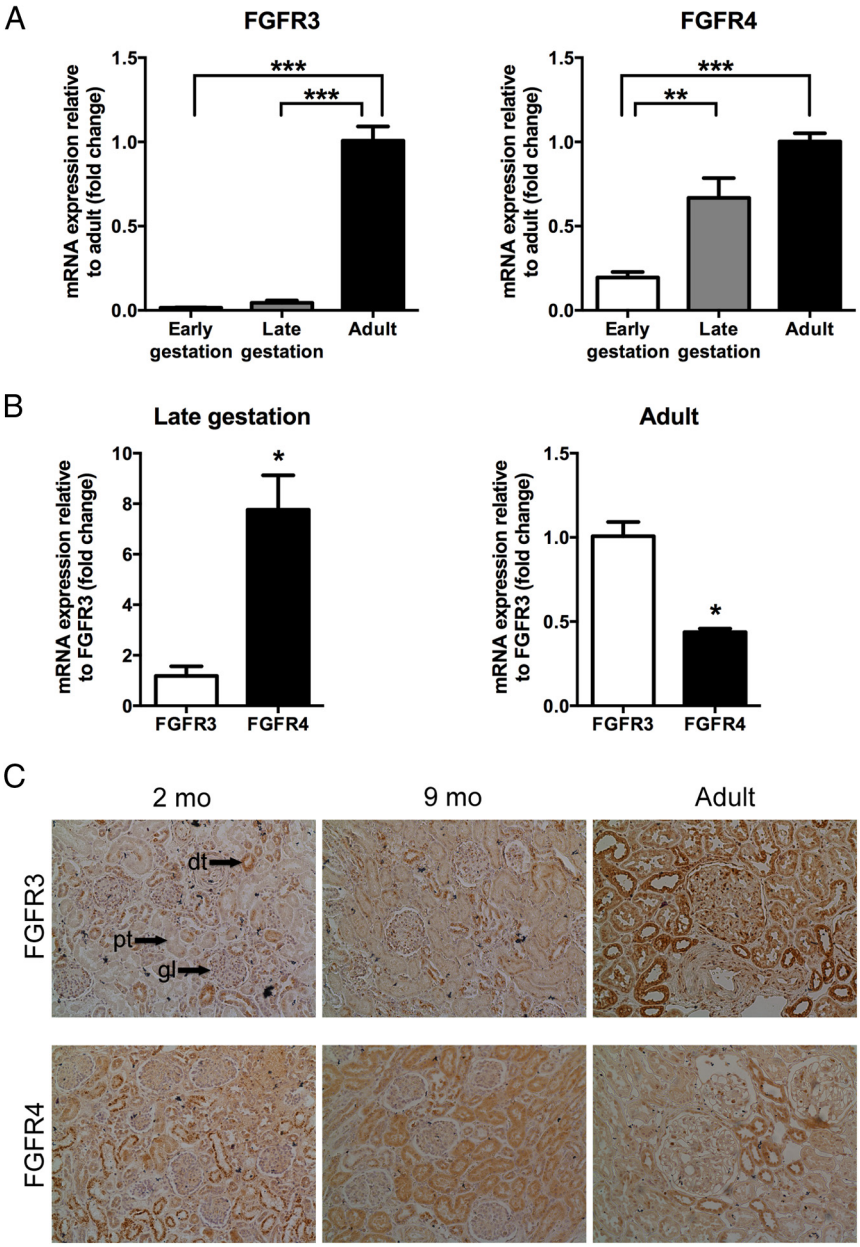

Figure 4. Renal FGFR expression in fetal, neonatal, and adult tissue. *FGFR* gene expression was studied using RT-qPCR. A, Expression of *FGFR*s in fetal (early GA of 14–16 wk; late GA of 38–40 wk) and adult renal tissues. Relative expression was calculated with the $2^{-\Delta\Delta CT}$ method. Data are expressed as fold change relative to adult values. Statistical analysis was performed via one-way ANOVA followed by Bonferroni's multiple comparison test. B, *FGFR4* expression in fetal (late, GA of 38–40 wk) and adult tissue as compared with *FGFR3*. Relative expression was calculated with the $2^{-\Delta\Delta CT}$ method. Data are expressed as fold change relative to *FGFR3* levels. Statistical analysis was performed via an unpaired Student's *t* test. Results are presented as mean ± SEM of two independent determinations performed in duplicate. ***, $P < .0005$; **, $P < .008$; *, $P < .004$. C, Immunostaining of FGFRs in neonatal and adult kidney tissue (60 y of age). Magnification, ×20. Arrows indicate a typical example of a glomerulus (gl), proximal tubule (pt), and distal tubule (dt).

Our study is one of the first to provide a detailed description of human renal FGFR ontogeny. Cancilla et al (24) demonstrated that *FGFR3* and *FGFR4* gene expression could be detected in the developing rat kidney and increased during development. Furthermore, at embryonic day 20, FGFR3 protein expression was present in the distal tubules, whereas immunostaining was absent in the proximal tubules. In contrast, FGFR4 immunoreactivity was present in both distal and proximal tubules (24). This expression pattern is similar to our observations. In addition, other studies have also demonstrated the expression of *FGFR4* during renal development in rat and mice (25, 26), and recently it was reported in a zebrafish study that *fgf23* and *αklotho* were continuously expressed in the developing kidney (27). Several decades ago, Partanen et al (28) reported the expression of both *FGFR3* and *FGFR4* in the human fetal kidney (GA 17–18 wk), and they described that organ-specific *FGFR4* expression highly differs from other FGFRs. In a follow-up study, they investigated the expression of FGFR4 in the developing mouse, and, similar to our findings, they demonstrated that the *Fgfr4* gene expression in the murine embryo steadily increased during development and was hardly detectable in newborn and 2-day-old mice (29). Clearly, temporal FGFR expression is conserved among species and is subjected to change during both early renal development and aging.

The present study has some drawbacks. First of all, calcium homeostasis is a complex system involving a myriad of negative feedback loops and multiple hormones (10), but unfortunately, during the early clinical investigations, serum levels of FGF23, soluble Klotho, and active vitamin D have not been determined. Second, we could not get access to mRNA from early postnatal kidneys, limiting the latter part of our study solely to protein expression. Still, this study is the first to concisely describe postnatal serum calcium levels in an individual with Sotos syndrome, and owing to the availability of a unique and precious human kidney collection, we have been able to partially dissect and elucidate the expression profile of FGFRs during human renal development.

In conclusion, we have demonstrated the presence of transient infantile hypercalcemia in a 5q35 microdeletion case of Sotos syndrome, which included a deletion of *FGFR4*. Furthermore, we found that FGFR4 is highly ex-

pressed in fetal and neonatal kidney, whereas FGFR3 expression is highest in adult tissue. This indicates that there is a developmental switch in the contribution of both FGFRs to FGF23 signaling during aging, which could explain the fleeting hypercalcemia. These findings provide a novel and intriguing insight into FGF23-mediated calcium homeostasis.

Acknowledgments

We thank Anne-Lise Delezoide (Robert-Debré University Hospital, Paris, France) for providing us with renal samples. The help of Jitske Jansen is also highly appreciated.

Address all correspondence and requests for reprints to: Dr M. Lombès, Institut National de la Santé et de la Recherche Médicale, Unité 693, Faculté de Médecine Paris-Sud, 63 Rue Gabriel Péri, 94276 Le Kremlin-Bicêtre, France. E-mail: marc.lombes@u-psud.fr.

This work was supported by the European Renal Association-European Dialysis and Transplant Association (Fellowship ERA STF 132–2013; www.era-edta.org) and by support from the Institut National de la Santé et de la Recherche Médicale and Université Paris Sud. E.N.L. and K.A. are supported by the Fund for Scientific Research, Flanders, Belgium (FWO Vlaanderen; Grants 1801110N and 1800214N, respectively).

Disclosure Summary: The authors have nothing to disclose.

References

1. **Sotos JF, Dodge PR, Muirhead D, Crawford JD, Talbot NB.** Cerebral gigantism in childhood. A syndrome of excessively rapid growth and acromegalic features and a nonprogressive neurologic disorder. *N Engl J Med*. 1964;271:109–116.
2. **Cole TR, Hughes HE.** Sotos syndrome: a study of the diagnostic criteria and natural history. *J Med Genet*. 1994;31:20–32.
3. **Tatton-Brown K, Rahman N.** Sotos syndrome. *Eur J Hum Genet*. 2007;15:264–271.
4. **Baujat G, Cormier-Daire V.** Sotos syndrome. *Orphanet J Rare Dis*. 2007;2:36.
5. **Tatton-Brown K, Douglas J, Coleman K, et al.** Multiple mechanisms are implicated in the generation of 5q35 microdeletions in Sotos syndrome. *J Med Genet*. 2005;42:307–313.
6. **Saugier-Veber P, Bonnet C, Drouin-Garraud V, et al.** Heterogeneity of NSD1 alterations in 116 patients with Sotos syndrome. *Hum Mutat*. 2007;28:1098–1107.
7. **Kenny J, Lees MM, Drury S, et al.** Sotos syndrome, infantile hypercalcemia, and nephrocalcinosis: a contiguous gene syndrome. *Pediatr Nephrol*. 2011;26:1331–1334.
8. **Magen D, Berger L, Coady MJ, et al.** A loss-of-function mutation in NaPi-IIa and renal Fanconi's syndrome. *N Engl J Med*. 2010;362:1102–1109.
9. **Beck L, Karaplis AC, Amizuka N, Hewson AS, Ozawa H, Tenenhouse HS.** Targeted inactivation of Npt2 in mice leads to severe renal phosphate wasting, hypercalciuria, and skeletal abnormalities. *Proc Natl Acad Sci USA*. 1998;95:5372–5377.
10. **Hu MC, Shiizaki K, Kuro-o M, Moe OW.** Fibroblast growth factor 23 and Klotho: physiology and pathophysiology of an endocrine network of mineral metabolism. *Annu Rev Physiol*. 2013;75:503–533.
11. **Nabeshima Y.** Discovery of α-Klotho unveiled new insights into calcium and phosphate homeostasis. *Proc Jpn Acad Ser B Phys Biol Sci*. 2009;85:125–141.
12. **Kurosu H, Ogawa Y, Miyoshi M, et al.** Regulation of fibroblast growth factor-23 signaling by klotho. *J Biol Chem*. 2006;281:6120–6123.
13. **Gattineni J, Bates C, Twombley K, et al.** FGF23 decreases renal NaPi-2a and NaPi-2c expression and induces hypophosphatemia in vivo predominantly via FGF receptor 1. *Am J Physiol Renal Physiol*. 2009;297:F282–F291.
14. **Gattineni J, Twombley K, Goetz R, Mohammadi M, Baum M.** Regulation of serum 1,25(OH)2 vitamin D3 levels by fibroblast growth factor 23 is mediated by FGF receptors 3 and 4. *Am J Physiol Renal Physiol*. 2011;301:F371–F377.
15. **Martinerie L, Viengchareun S, Delezoide AL, et al.** Low renal mineralocorticoid receptor expression at birth contributes to partial aldosterone resistance in neonates. *Endocrinology*. 2009;150:4414–4424.
16. **Levtchenko E, Schoeber J, Jaeken J.** Genetic disorders of renal phosphate transport. *N Engl J Med*. 2010;363:1774; author reply 1774–1775.
17. **Gattineni J, Baum M.** Regulation of phosphate transport by fibroblast growth factor 23 (FGF23): implications for disorders of phosphate metabolism. *Pediatr Nephrol*. 2010;25:591–601.
18. **Tatton-Brown K, Douglas J, Coleman K, et al.** Genotype-phenotype associations in Sotos syndrome: an analysis of 266 individuals with NSD1 aberrations. *Am J Hum Genet*. 2005;77:193–204.
19. **Shimada T, Kakitani M, Yamazaki Y, et al.** Targeted ablation of Fgf23 demonstrates an essential physiological role of FGF23 in phosphate and vitamin D metabolism. *J Clin Invest*. 2004;113:561–568.
20. **Yuan Q, Sitara D, Sato T, et al.** PTH ablation ameliorates the anomalies of Fgf23-deficient mice by suppressing the elevated vitamin D and calcium levels. *Endocrinology*. 2011;152:4053–4061.
21. **Kuro-o M, Matsumura Y, Aizawa H, et al.** Mutation of the mouse klotho gene leads to a syndrome resembling ageing. *Nature*. 1997;390:45–51.
22. **Nakatani T, Sarraj B, Ohnishi M, et al.** In vivo genetic evidence for klotho-dependent, fibroblast growth factor 23 (Fgf23)-mediated regulation of systemic phosphate homeostasis. *FASEB J*. 2009;23:433–441.
23. **Haenzi B, Bonny O, Masson R, et al.** Loss of Memo, a novel FGFR regulator, results in reduced lifespan. *FASEB J*. 2014;28(1):327–336.
24. **Cancilla B, Ford-Perriss MD, Bertram JF.** Expression and localization of fibroblast growth factors and fibroblast growth factor receptors in the developing rat kidney. *Kidney Int*. 1999;56:2025–2039.
25. **Ford MD, Cauchi J, Greferath U, Bertram JF.** Expression of fibroblast growth factors and their receptors in rat glomeruli. *Kidney Int*. 1997;51:1729–1738.
26. **Cool SM, Sayer RE, van Heumen WR, Pickles JO, Nurcombe V.** Temporal and spatial expression of fibroblast growth factor receptor 4 isoforms in murine tissues. *Histochem J*. 2002;34:291–297.
27. **Mangos S, Amaral AP, Faul C, Juppner H, Reiser J, Wolf M.** Expression of fgf23 and αklotho in developing embryonic tissues and adult kidney of the zebrafish, *Danio rerio*. *Nephrol Dial Transplant*. 2012;27:4314–4322.
28. **Partanen J, Makela TP, Claesson-Welsh L, et al.** FGFR-4, a novel acidic fibroblast growth factor receptor with a distinct expression pattern. *EMBO J*. 1991;10:1347–1354.
29. **Korhonen J, Partanen J, Alitalo K.** Expression of FGFR-4 mRNA in developing mouse tissues. *Int J Dev Biol*. 1992;36:323–329.